Phytochemistry Letters 70 (2025) 104061

Contents lists available at ScienceDirect

Phytochemistry Letters

journal homepage: www.elsevier.com/locate/phytol

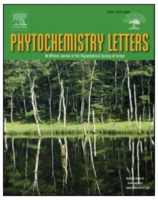

ent-Kaurane derivatives from *Smallanthus sonchifolius*

Pham Thi Mai Huong [a,b], Pham Thi Cham [a], Le Thi Vien [a], Tran Thi Hong Hanh [a,*], Nguyen The Cuong [c], Nguyen Xuan Cuong [a,*], Nguyen Hoai Nam [a]

[a] *Institute of Chemistry, Vietnam Academy of Science and Technology (VAST), 18 Hoang Quoc Viet, Nghia Do, Hanoi, Viet Nam*
[b] *Faculty of Pharmacy, Thanh Do University, Kim Chung, Hoai Duc, Hanoi, Viet Nam*
[c] *Institute of Biology, VAST, 18 Hoang Quoc Viet, Nghia Do, Hanoi, Viet Nam*

ARTICLE INFO

Keywords:
Smallanthus sonchifolius
Asteraceae
ent-kaurane derivative
α-glucosidase inhibition

ABSTRACT

Phytochemical study of *Smallanthus sonchifolius* tubers led to the isolation of seven *ent*-kaurane derivatives, including three new compounds, namely sonchifoliosides A–C (**1**–**3**). Their structures were confirmed by a detailed analysis of the 1D and 2D NMR and HR-ESI-QTOF mass spectra. Among the isolates, 16α,17,19-trihydroxy-*ent*-kaurane 19-*O*-β-D-glucopyranoside (**5**) exhibited α-glucosidase inhibitory activity with an IC_{50} value of 104.71 ± 0.45 μM.

1. Introduction

The *ent*-kaurane diterpenes are a class of typical tetracyclic diterpenoids, being considered as intermediates of the plant hormones gibberellins. Structurally, these compounds are constituted by a perhydrophenanthrene unit (rings A, B, and C) fused with a cyclopentane (ring D). These diterpenes are naturally found in various plants, having potential biological effects such as neuroprotective, anti-inflammatory, and cytotoxic effects (García et al., 2007; Qi et al., 2018).

Within the frame of our investigations on *ent*-kaurane constituents from Vietnamese medicinal plants, stevibioside A was recently reported from *Stevia rebaudiana*, exhibiting potent α-glycosidase inhibitory activity with IC_{50} value of 8.9 ± 0.45 μM. In addition, this *ent*-kaurane glycoside revealed uncompetitive mode of inhibition with *K*i value of 2.18 ± 0.81 μM (Hanh et al., 2024). In line with this, the current paper addresses the isolation and structure elucidation of seven *ent*-kaurane derivatives from *Smallanthus sonchifolius* tubers. Their α-glucosidase inhibitory effects were also evaluated.

2. Results and discussion

Seven *ent*-kaurane derivatives (**1**–**7**, Fig. 1) were isolated from *S. sonchifolius* tubers by using various chromatographic experiments. Extensive analysis of the 1D and 2D NMR data in comparison with the literature values led to identification of known compounds as paniculoside IV (**4**) (Yamasaki et al., 1977), 16α,17,19-trihydroxy-*ent*-kaurane 19-*O*-β-D-glucopyranoside (**5**) (Satake et al., 1983), sylvestriside A (**6**) (Wang et al., 2009), 3β,16α,17-trihydroxy-*ent*-kauran-19-oic-acid (**7**) (Ohkoshi et al., 2004).

Compound **1** was isolated as a white amorphous powder. Its molecular formula was identified as $C_{30}H_{46}O_{10}$ by the HR-QTOF-MS with a quasi-molecular ion peak at *m/z* 601.2754 $[M+Cl]^-$. ^1H and ^{13}C NMR spectra revealed typical signals of an isobutyroyl moiety at δ_C 178.6 (C-1′), 35.7 (C-2′), 19.3 (C-3′), and 19.4 (C-4′)/δ_H 2.54 (1 H, qu, *J* = 7.0 Hz, H-2′), 1.16 (3 H, d, *J* = 7.0 Hz, H-3′), and 1.17 (3 H, d, *J* = 7.0 Hz, H-4′) (Veneziani et al., 1999) and a β-D-glucopyranosyl unit at δ_C 95.6 (C-1″), 74.1 (C-2″), 78.7 (C-3″), 71.2 (C-4″), 78.7 (C-5″), and 62.4 (C-6″)/δ_H 5.44 (1 H, d, *J* = 8.0 Hz, H-1″) (Tan et al., 1993). With 20 carbon atoms including typical signals of one carbonyl carbon [δ_C 178.5 (C-19)] and a 1,1-disubstituted double bond [δ_C 157.7 (C-16) and 110.1 (C-17)/δ_H 5.07 (1 H, s, H_a-17) and 5.10 (1 H, s, H_b-17)], the aglycone of **1** was suggested to have an *ent*-16-kauren-19-oic acid skeleton, one main constituents of *Smallanthus* species (Coll Aráoz et al., 2010). In addition, the signals of one quaternary oxygenated carbon [δ_C 77.8 (C-9)], one oxymethine [δ_C 80.5 (C-15)/δ_H 5.97 (br s, H-15)], and two tertiary methyls [δ_C 29.1 (C-18) and 18.2 (C-20)/δ_H 1.25 (H-18) and 1.12 (H-20), each 3 H, s] were also observed. The HMBC cross-peaks of H-20 (δ_H 1.12) with C-1 (δ_C 33.3), C-5 (δ_C 51.2), and C-9 (δ_C 77.8); H-15 (δ_H 5.97) with C-9 (δ_C 77.8); and those of H-17 (δ_H 5.07 and 5.10) with C-13 (δ_C 42.7) and C-15 (δ_C 80.5) clearly confirmed locations of the quaternary oxygenated carbon C-9 and oxymethine C-15 (Fig. 2). HMBC interactions were also observed between H-15 (δ_H 5.97) and C-1′ (δ_C

---

* Corresponding authors.
E-mail addresses: tranhonghanh@ich.vast.vn (T.T.H. Hanh), cuongnx@ich.vast.vn (N.X. Cuong).

https://doi.org/10.1016/j.phytol.2025.104061
Received 19 April 2025; Received in revised form 12 October 2025; Accepted 15 October 2025

178.6) as well as H-1″ (δ_H 5.44) and C-19 (δ_C 178.5) confirming esterification of the isobutyroyl and *β*-D-glucopyranosyl moieties at C-15 and C-19, respectively. The ^{1}H and ^{13}C NMR data for the aglycone of **1** were essentially identical to those of *β*-D-glucopyranosyl-15*α*-[(2-methylbutanoyl)oxy]-9-*β*-hydroxy-*ent*-16-kauren-19-oate (Dong et al., 2017), suggesting that these two compounds have same configurations. The negative specific rotation (−24) of **1** further confirmed the *ent*-kaurane structure (Qi et al., 2018). This was aslo supported by the experimental ECD spectrum, which showed a strong negative Cotton effect at 209 nm, in comparison with the calculated spectra (using Gaussian16W, Revision C.01, Gaussian, Inc, Wallingford, CT, employing the B3LYP/6–31 g(d,p) level for MeOH with the IEFPCM model) for both the *ent*-kaurane (**1a**) and kaurane (**1b**) forms of the aglycone of **1** (Fig. 3), following previously described procedures (Ngoc et al., 2022). Moreover, NOESY interactions of H-5 (δ_H 1.70) with H$_\beta$-7 (δ_H 1.60) and H-18 (δ_H 1.25) as well as H$_\beta$-7 (δ_H 1.60) with H-15 (δ_H 5.97) unambiguously indicated *β*-orientation of H-15 and the methyl group at C-4 (Fig. 2). Thus, the structure of **1** was elucidated as *β*-D-glucopyranosyl-15*α*-isobutyroyl-9*β*-hydroxy-*ent*-16-kauren-19-oate and named sonchifolioside A.

The ^{1}H and ^{13}C NMR data of **2** were similar to those of **1** (see Table 1), except for presence of a quaternary oxygenated carbon [δ_C 67.9 (C-16)] and an oxymethylene [δ_C 50.4 (C-17)/δ_H 2.79 and 3.01 (each 1 H, d, $J = 6.0$ Hz, H-17)] in **2** replaced for the 1,1-disubstituted double bond in **1**. HMBC cross-peak of H-15 (δ_H 5.43) with C-17 (δ_C 50.4) clearly confirmed positions of the quaternary oxygenated carbon C-16 and the oxymethylene C-17. The carbon signals of C-16 and C-17 of **2** were strongly shifted upfield relative to those of paniculoside IV (Yamasaki et al., 1977) confirming presence of an epoxy bridge at C-16/C-17 (Sebisubi et al., 2010; Yang et al., 2007). This was further confirmed by HR-QTOF-MS with a quasi-molecular ion peak at *m/z* 617.2720 [M+Cl]$^-$, consistent with the molecular formula of **2** as $C_{30}H_{46}O_{11}$. Consequently, the structure *β*-D-glucopyranosyl-15*α*-isobutyroyl-9*β*-hydroxy-16,17-epoxy-*ent*-kauran-19-oate was confirmed for **2** and named sonchifolioside B.

The ^{1}H and ^{13}C NMR data of **3** were similar to those of **2** (see Table 1), except for presence of an angeloyl moiety [δ_C 169.5 (C-1′), 129.6 (C-2′), 137.7 (C-3′), 15.9 (C-4′), and 20.8 (C-5′)/δ_H 6.07 (1 H, ddd, $J = 7.0$, 1.5, 1.5 Hz, H-3′), 1.96 (1 H, dd, $J = 7.0$, 1.5 Hz, H-4′), and 1.89 (1 H, t, $J = 1.5$ Hz, H-5′)] (Wafo et al., 2011) in **3** replaced for the isobutyroyl unit in **2**. This was also supported by HR-QTOF-MS with a quasi-molecular ion peak at *m/z* 617.2910 [M+Na]$^+$. Location of the angeloyl moiety at C-15 was indicated by HMBC cross-peak of H-15 (δ_H 5.55) with C-1′ (δ_C 169.5). Thus, **3** was elucidated as *β*-D-glucopyranosyl-15*α*-angeloyl-9*β*-hydroxy-16,17-epoxy-*ent*-kauran-19-oate and named sonchifolioside C.

Isolated compounds were evaluated for their α-glucosidase inhibitory effects following previously described steps (Hanh et al., 2024). As the obtained results, only 16*α*,17,19-trihydroxy-*ent*-kaurane 19-*O*-*β*-D-glucopyranoside (**5**) exhibited activity with an IC$_{50}$ value of 104.71 ± 0.45 μM, relative to that of the positive control acarbose (IC$_{50}$ = 46.78 ± 1.56 μM). Other compounds were less active at concentrations up to 200 μM.

3. Experimental

3.1. General experimental procedures

The optical rotations were determined on a JASCO P-2000

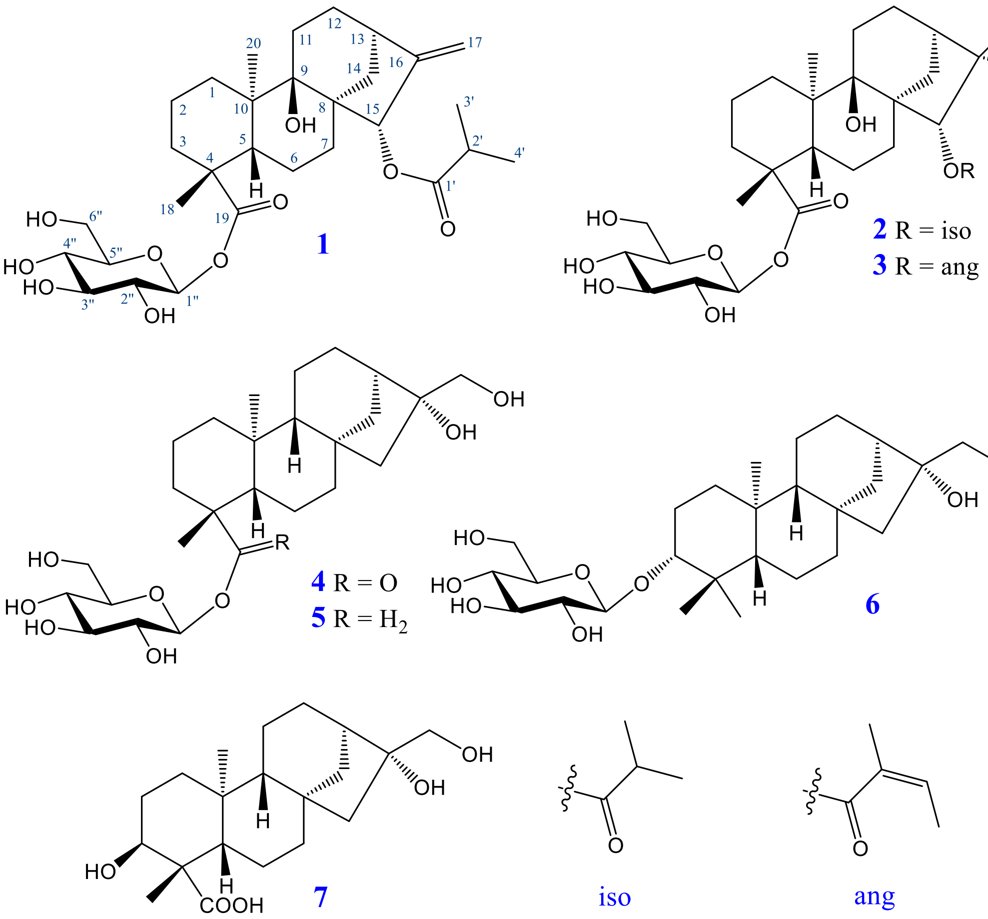

Fig. 1. The structures of compounds **1**—**7**.

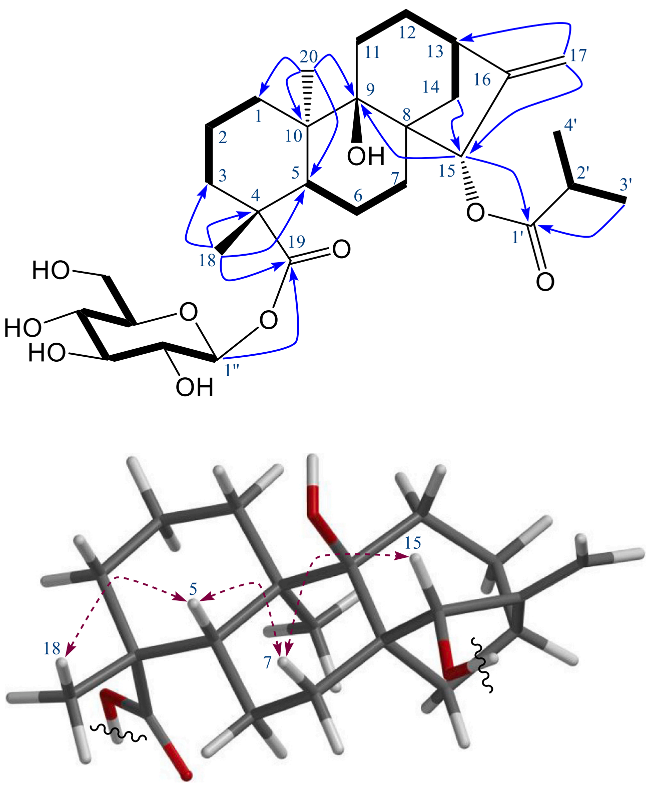

Fig. 2. Key HMBC (⟶), COSY (▬), and NOESY (⤻) correlations of **1**.

polarimeter (Tokyo, Japan). CD spectra were recorded with an Applied Photophysics Chirascan spectrometer (Surrey, United Kingdom). The high-resolution mass spectra were recorded on an Agilent 6530 Accurate-Mass spectrometer (CA, USA). The ^{1}H NMR and ^{13}C NMR spectra were recorded on a Bruker AVANCE III HD 500 FT-NMR spectrometer (Karlsruhe, Germany) with TMS used as an internal standard. Column chromatography (CC) was performed on silica gel (Kieselgel 60, 70–230 mesh and 230–400 mesh, Merck), reversed-phase silica gel (ODS-A, 12 nm S-150 µm, YMC Co., Ltd.), Sephadex LH-20 (Sigma), and Diaion HP-20 (Supelco) resins. Medium pressure liquid chromatography (MPLC) was carried out on a Biotage - Isolera One system (SE-751 03 Uppsala, Sweden). HPLC purification was carried out on an Agilent 1260 Infinity II system equipped with a G7112B Binary Pump, a G7115A diode array detector, and a G7129A auto-sampler). TLC used precoated silica gel 60 F_{254} (Merck) and RP-18 F_{254S} plates (Merck), and the spots were visualized by spraying with aqueous 10 % H_2SO_4, which was followed by heating for 3–5 min. ECD calculations were carried out on Dell Precision 5820 systems equipped with an Intel Xeon W-2175 2.50 GHz processor, 32 GB RAM, and Windows 11 Pro for Workstations.

3.2. *Plant material*

The *Smallanthus sonchifolius* (Poepp.) H.Rob. (Asteraceae) samples were collected at Bat Xat, Lao Cai, Vietnam, in May 2024. The voucher specimen (No: SS.5.2024) was identified by Dr. Nguyen The Cuong and deposited at the Institute of Biology, VAST, Vietnam.

3.3. *Extraction and isolation*

The *S. sonchifolius* tubers were dried (3 kg), powdered, and extracted with MeOH (3 ×3 L) under ultrasonic conditions (1 h each) to obtain the MeOH extract (M, 500 g). Extract M was suspended in water (2 L) and partitioned in turn with *n*-hexane, CH_2Cl_2, and EtOAc to obtain the *n*-hexane (H, 70 g), CH_2Cl_2 (D, 25), EtOAc (E, 15) extracts and water layer. Extracts D (25 g) and E (15 g) were combined and separated into six fractions, D1-D6, using silica gel MPLC with mobile phase of CH_2Cl_2–MeOH (gradient 100:1→1:100, v/v). Fraction D3 (4 g) was further separated on RP-18 MPLC with MeOH–H_2O (gradient 10:10→10:1, v/v) to obtain seven subfractions, D3A-D3G. Subfraction D3C (51 mg) was divided into two smaller fractions, D3C1 (20 mg) and D3C2 (30 mg), using Shephadex LH-20 CC with MeOH–H_2O (1:1, v/v). Purification of D3C1 (20 mg) on HPLC (column: Cosmosil 5C18-MS-II, 250 × 20 mm, 5 µm; flow rate: 2.5 ml/min; MeOH–H_2O 55:45) obtained **2** (1.6 mg). Fraction D3C2 (30 mg) was treated by the same

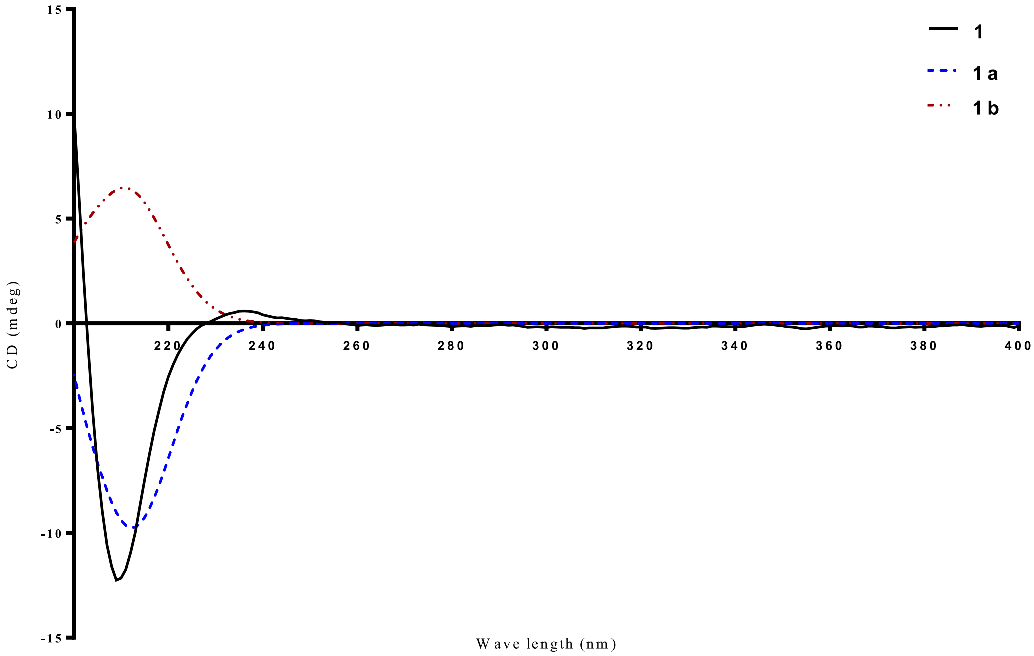

Fig. 3. Experimental ECD spectrum of **1** and calculated spectra for the *ent*-kaurane (**1a**) and kaurane (**1b**) forms of its aglycone.

Table 1
^1H and ^{13}C NMR spectroscopic data of **1**–**3** in CD_3OD.

No	**1**		**2**		**3**	
	δ_C[a]	δ_H[b] mult. (*J* in Hz)	δ_C[a]	δ_H[b] mult. (*J* in Hz)	δ_C[a]	δ_H[b] mult. (*J* in Hz)
1	33.3	1.50 m/ 1.78 m	33.4	1.53 m/ 1.80 m	33.4	1.53 m/ 1.80 m
2	20.1	1.45 m/ 1.97 m	20.0	1.50 m/ 2.00 m	20.2	1.50 m/ 2.00 m
3	38.7	1.08 m/ 2.17 m	38.8	1.08 m/ 2.17 m	38.8	1.08 m/ 2.18 m
4	45.2	-	45.2	-	45.2	-
5	51.2	1.70 dd (13.0, 2.0)	51.1	1.73 dd (12.5, 2.0)	51.1	1.75 m
6	22.0	1.86 m/ 2.02 m	21.9	1.90 m/ 2.10 m	22.0	1.89 m/ 2.10 m
7	31.0	1.50 m/ 1.60 m	31.1	1.65 m	31.4	1.65 m
8	54.1	-	54.7	-	54.7	-
9	77.8	-	77.3	-	77.3	-
10	45.7	-	45.7	-	45.7	-
11	29.5	1.27 m/ 2.00 m	30.9	1.31 m/ 2.17 m	31.0	1.32 m/ 2.20 m
12	34.9	1.57 m/ 1.74 m	30.8	1.68 m	30.8	1.69 m
13	42.7	2.74 br s	41.5	1.79 br s	41.5	1.81 br s
14	38.7	1.55 m/2.28 br d (12.5)	37.8	1.80 m/2.34 br d (11.5)	38.0	1.82 m/2.36 br d (11.0)
15	80.5	5.97 br s	79.3	5.43 br s	79.4	5.55 br s
16	157.7	-	67.9	-	68.0	-
17	110.1	5.07 s/5.10 s	50.4	2.79 d (6.0)/ 3.01 d (6.0)	50.5	2.81 d (6.0)/ 3.08 d (6.0)
18	29.1	1.25 s	29.1	1.26 s	29.1	1.26 s
19	178.5	-	178.6	-	178.6	-
20	18.2	1.12 s	18.3	1.14 s	18.3	1.15 s
Iso					*Ang*	
1′	178.6	-	178.6	-	169.5	-
2′	35.7	2.54 qu (7.0)	35.4	2.56 qu (7.0)	129.6	-
3′	19.3	1.16 d (7.0)	19.5	1.17 d (7.0)	137.7	6.07 ddd (7.0, 1.5, 1.5)
4′	19.4	1.17 d (7.0)	19.5	1.17 d (7.0)	15.9	1.96 dd (7.0, 1.5)
5′					20.8	1.89 t (1.5)
Glc						
1″	95.6	5.44 d (8.0)	95.6	5.44 d (8.0)	95.6	5.44 d (8.0)
2″	74.1	3.40 m	74.1	3.40 m	74.1	3.40 m
3″	78.7	3.40 m	78.8	3.40 m	78.8	3.40 m
4″	71.2	3.40 m	71.2	3.40 m	71.1	3.40 m
5″	78.7	3.41 m	78.8	3.41 m	78.8	3.41 m
6″	62.4	3.71 dd (12.0, 4.5) 3.86 dd (12.0, 1.5)	62.4	3.70 dd (12.0, 4.5) 3.86 dd (12.0, 1.5)	62.4	3.71 dd (12.0, 4.0) 3.85 br d (12.0)

[a] 125 MHz.
[b] 500 MHz.

manner as D3C1 to yield **3** (5.5 mg). Subfraction D3E (32 mg) was purified on Shephadex LH-20 CC with $MeOH-H_2O$ (1:1, v/v) and then on silica gel CC with CH_2Cl_2–acetone (1:1.5, v/v) to give **1** (2.1 mg). Fraction D5 (7.5 g) was further separated on silica gel CC with $CH_2Cl_2-MeOH-H_2O$ (6:1:0.05, v/v) to give six subfractions, D5A-D5F. Subfraction D5E (1.1 g) was divided into five smaller fractions, D5E1-D5E5, using reverse phase silica gel CC with acetone–H_2O (1:1.5, v/v). Compounds **4** (3.5 mg) and **5** (2.2 mg) were purified from fraction D5E4 (120 mg) after subjecting it to silica gel CC with $CH_2Cl_2-MeOH-H_2O$ (5:1:0.1, v/v). Subfraction D5F (0.9 g) was divided into four smaller fractions, D5F1-D5F4, using silica gel CC with $CH_2Cl_2-MeOH-H_2O$ (5:1:0.05, v/v). Purification of D5F2 (55 mg) on Shephadex LH-20 CC with $MeOH-H_2O$ (1:1, v/v) and then on HPLC (column: Cosmosil 5C18-MS-II, 250 × 20 mm, 5 μm; flow rate: 2.5 ml/min; $MeOH-H_2O$ 48:52) obtained **6** (5.5 mg). Similarly, **7** (4.0 mg) was purified from D3F3 (65 mg) after subjecting it to Shephadex LH-20 CC with $MeOH-H_2O$ (1:1, v/v) and then on HPLC (column: Cosmosil 5C18-MS-II, 250 × 20 mm, 5 μm; flow rate: 2.5 ml/min; $ACN-H_2O$ 29:71).

3.3.1. *Sonchifolioside A (1)*

White amorphous powder, $[\alpha]_D^{20} = -24.0$ (*c* 0.08, MeOH); CD (MeOH) λ_{max} (mdeg): 209 (−12.26) and 236 (+0.58) nm; ^1H (CD_3OD, 500 MHz) and ^{13}C NMR (CD_3OD, 125 MHz) data are given in Table 1; HR-QTOF-MS *m/z* 601.2754 $[M+Cl]^-$ (calcd. for $C_{30}H_{46}ClO_{10}^-$, 601.2785).

3.3.2. *Sonchifolioside B (2)*

White amorphous powder, $[\alpha]_D^{20} = -20.0$ (*c* 0.05, MeOH); CD (MeOH) λ_{max} (mdeg): 215 (−2.75) and 238 (+1.16) nm; ^1H (CD_3OD, 500 MHz) and ^{13}C NMR (CD_3OD, 125 MHz) data are given in Table 1; HR-QTOF-MS *m/z* 617.2720 $[M+Cl]^-$ (calcd. for $C_{30}H_{46}ClO_{11}^-$, 617.2734).

3.3.3. *Sonchifolioside C (3)*

White amorphous powder, $[\alpha]_D^{20} = -47.0$ (*c* 0.05, MeOH); CD (MeOH) λ_{max} (mdeg): 221 (−5.35) and 243 (+4.94) nm; ^1H (CD_3OD, 500 MHz) and ^{13}C NMR (CD_3OD, 125 MHz) data are given in Table 1; HR-QTOF-MS *m/z* 617.2910 $[M+Na]^+$ (calcd. for $C_{31}H_{46}NaO_{11}^+$, 617.2932).

3.4. *α-Glucosidase inhibitory assay*

α-Glucosidase inhibitory assay was carried out using the previously described method (Bharadwaj et al., 2018) with slight modifications (Hanh et al., 2024). Briefly, compounds **1-7** were dissolved in DMSO at 10 mg/ml stock concentration and diluted with phosphate buffer pH 6.8 to the desired concentration. The reaction mixture in a 96 wells plate contained 50 *μ*L of samples at different concentrations and 100 *μ*L (0.1 units/ml) of *α*-glucosidase enzyme from *Saccharomyces cerevisiae* E.C 3.2.1.20 (19.3 U/mg, G5003, Sigma, USA). The reaction mixture was incubated at 37 °C for 10 min. Then, 50 *μ*L of *p*-nitrophenyl-*α*-D-glucopyranoside (*p*-NPG, 5 mM, Sigma, USA) was added to the reaction mixture and incubated at 37 °C for 30 min. Immediately preceding analysis, 100 *μ*L of sodium carbonate (200 mM) solution was added to the reaction mixture to retard the enzyme activity. The blank for the reaction was prepared by replacing the sample and enzyme with buffer. Similarly, the control was prepared using a buffer in place of the sample. Also, blank solutions were prepared for each sample by replacing an enzyme with a buffer. The absorbance of *p*-nitrophenol released during the reaction was quantified by reading at 405 nm using the microreader (Epoch, Biotek, USA). Acarbose was used as a positive control for the assay. The percentage of *α*-glucosidase enzyme inhibition was calculated using the following formula:

$$\text{Inhibition}(\%) = \left[1 - \frac{A_{\text{sample}}}{A_{\text{control}}}\right] \times 100$$

where % inhibition is the percentage of inhibition, A_{sample} is the corrected absorbance of the extracts or isolated compounds under testing $[A_{\text{sample(initial)}} - A_{\text{blank-sample}} - A_{\text{blank-plate}}]$, and A_{control} is the absorbance of the negative control $[A_{\text{negative-control-(initial)}} - A_{\text{blank-plate}}]$. The half-maximal inhibitory concentration (IC_{50}) was calculated as the compound concentration that is required for 50 % inhibition using GraphPad Prism version 6.0 for Windows (GraphPad Software).

CRediT authorship contribution statement

Tran Thi Hong Hanh: Writing – review & editing, Data curation. **Le Thi Vien:** Investigation. **Pham Thi Cham:** Investigation. **Pham Thi Mai Huong:** Writing – original draft, Investigation. **Nguyen Hoai Nam:** Writing – review & editing, Supervision. **Nguyen Xuan Cuong:** Writing – review & editing, Data curation. **Nguyen The Cuong:** Investigation.

Declaration of Competing Interest

The authors declare that they have no known competing financial interests or personal relationships that could have appeared to influence the work reported in this paper.

Acknowledgements

This research is financially supported by Vietnam Academy of Science and Technology (VAST) under grant number THTETN.07/24-25.

Appendix A. Supporting information

Supplementary data associated with this article can be found in the online version at doi:10.1016/j.phytol.2025.104061.

Data Availability

Data will be made available on request.

References

Bharadwaj, S.S., Poojary, B., Nandish, S.K.M., Kengaiah, J., Kirana, M.P., Shankar, M.K., Das, A.J., Kulal, A., Sannaningaiah, D., 2018. Efficient synthesis and in silico studies of the benzimidazole hybrid scaffold with the quinolinyloxadiazole skeleton with potential α-glucosidase inhibitory, anticoagulant, and antiplatelet activities for typeII diabetes mellitus management and treating thrombotic disorders. ACS Omega 3, 12562–12574.

Coll Aráoz, M.V., Mercado, M.I., Grau, A., Catalán, C.A.N., 2010. *Ent*-kaurane derivatives from the root cortex of yacon and other three *Smallanthus* species (Heliantheae, Asteraceae). Biochem. Syst. Ecol. 38, 1042–1048.

Dong, L.-M., Jia, X.-C., Luo, Q.-W., Peng, Y.-M., Zhang, Q., Luo, B., Tan, J.-W., 2017. Four new *ent*-kaurene diterpene glucosides from *Mikania micrantha*. Phytochem. Lett. 20, 155–159.

García, P.A., de Oliveira, A.B., Batista, R., 2007. Occurrence, biological activities and synthesis of kaurane diterpenes and their glycosides. Molecules 12, 455–483.

Hanh, T.T.H., Huong, P.T.M., Cham, P.T., Anh, D.H., Quang, T.H., Cuong, N.X., Nam, N. H., Minh, C.V., 2024. *ent*-kaurane glycosides from *Stevia rebaudiana* and their α-glucosidase inhibition. Tetrahedron 158, 133993.

Ngoc, N.T., Hanh, T.T.H., Quang, T.H., Cuong, N.X., Nam, N.H., Thao, D.T., Cuong, P.V., Thung, D.C., Kiem, P.V., Minh, C.V., 2022. Cembranoids from the Vietnamese soft coral *Sarcophyton ehrenbergi*. Nat. Prod. Res. 36, 5517–5523.

Ohkoshi, E., Kamo, S., Makino, M., Fujimoto, Y., 2004. *Ent*-Kaurenoic acids from *Mikania hirsutissima* (Compositae). Phytochemistry 65, 885–890.

Qi, X.L., Zhang, Y.Y., Zhao, P., Zhou, L., Wang, X.B., Huang, X.X., Lin, B., Song, S.J., 2018. *Ent*-Kaurane diterpenoids with neuroprotective properties from corn silk (*Zea mays*). J. Nat. Prod. 81, 1225–1234.

Satake, T., Murakami, T., Saiki, Y., Chen, C., 1983. Chemical and chemotaxonomical studies on filices. Xliii. chemical studies on the constituents of *Lindsaea javanensis* bl., *l. japonica* (Bak.) diels and *Tapeinidium pinnatum* (Cav.) C. Chr. Chem. Pharm. Bull. 31, 3865–3871.

Sebisubi, F.M., Odyek, O., Anokbonggo, W.W., Ogwal-Okeng, J., Carcache-Blanco, E.J., Ma, C., Orjala, J., Tan, G.T., 2010. Antimalarial activity of *Aspilia pruliseta*, a medicinal plant from Uganda. Planta Med. 76, 1870–1873.

Tan, R.X., Hu, Y.H., Liu, Z.L., Pan, X., 1993. New kaurane diterpenoids from *Aster tongolensis*. J. Nat. Prod. 56, 1917–1922.

Veneziani, R.C.S., Camilo, D., Oliveira, Rd, 1999. Constituents of *Mikania glomerata* sprengel. Biochem. Syst. Ecol. 27, 99–102.

Wafo, P., Kamdem, R.S., Ali, Z., Anjum, S., Begum, A., Oluyemisi, O.O., Khan, S.N., Ngadjui, B.T., Etoa, X.F., Choudhary, M.I., 2011. Kaurane-type diterpenoids from *Chromoleana odorata*, their X-ray diffraction studies and potent α-glucosidase inhibition of 16-kauren-19-oic acid. Fitoterapia 82, 642–646.

Wang, W., Zhao, J., Wang, Y.H., Smillie, T.A., Li, X.C., Khan, I.A., 2009. Diterpenoids from *Casearia sylvestris*. Planta Med 75, 1436–1441.

Yamasaki, K., Kohda, H., Kobayashi, T., Kaneda, N., Kasai, R., Tanaka, O., Nishi, K., 1977. Application of ^{13}C nuclear magnetic resonance spectroscopy to chemistry of glycosides: structures of paniculosides-I, -II, -III, -IV, and -V, diterpene glucosides of *Stevia paniculata* LAG. Chem. Pharm. Bull. 25, 2895–2899.

Yang, L.M., Hsu, F.L., Chang, S.F., Cheng, J.T., Hsu, J.Y., Hsu, C.Y., Liu, P.C., Lin, S.J., 2007. Microbial metabolism of steviol and steviol-16α,17-epoxide. Phytochemistry 68, 562–570.